OFFICE OF NAVAL RESEARCH

Grant No.

R&T Code N0014-92-C-0173

Technical Report #04

MOLECULAR DYNAMICS MODELING OF ELECTRIC DOUBLE LAYER

by

James N. Glosli
Michael R. Philpott

Prepared for publication

in the

Electrochemical Society Symposium Proceedings

IBM Research Division, Almaden Research Center,
650 Harry Road, San Jose, CA 95120-6099

1993

SECURITY CLASSIFICATION OF THIS PAGE *(When Data Entered)*

REPORT DOCUMENTATION PAGE		READ INSTRUCTIONS BEFORE COMPLETING FORM
1 REPORT NUMBER 04	2 GOVT ACCESSION NO	3 RECIPIENT'S CATALOG NUMBER
Technical Report 16 4 TITLE *(and Subtitle)* Molecular Dynamics Modeling of Electric Double Layers		5 TYPE OF REPORT & PERIOD COVERED Technical Report 6 PERFORMING ORG REPORT NUMBER
7 AUTHOR(s) James N. Glosli Michael R. Philpott		8 CONTRACT OR GRANT NUMBER(s) N00014-92-C-0173
9 PERFORMING ORGANIZATION NAME AND ADDRESS IBM Research Division, Almaden Research Center 650 Harry Road San Jose, CA 95120-6099		10 PROGRAM ELEMENT, PROJECT, TASK AREA & WORK UNIT NUMBERS
11 CONTROLLING OFFICE NAME AND ADDRESS Office of Naval Research 800 North Quincy Street Arlington, VA 22217		12 REPORT DATE 4/14/93 13 NUMBER OF PAGES 16
14 MONITORING AGENCY NAME & ADDRESS *(If different from Controlling Office)* Dr. Ronald A. De Marco Office of Naval Research, Chemistry Division 800 N. Quincy Street Arlington, VA 22217 U.S.A.		15 SECURITY CLASS *(of this report)* Unclassified 15a DECLASSIFICATION/DOWNGRADING SCHEDULE

16 DISTRIBUTION STATEMENT *(of this Report)*
Approved for public release; unlimited distribution.

17 DISTRIBUTION STATEMENT *(of the abstract entered in Block 20, if different from Report)*
Approved for public release; unlimited distribution.

18 SUPPLEMENTARY NOTES
Prepared for publication in Electrochemical Society Symposium Proceedings

19 KEY WORDS *(Continue on reverse side if necessary and identify by block number)*

20 ABSTRACT *(Continue on reverse side if necessary and identify by block number)*
SEE NEXT PAGE

SECURITY CLASSIFICATION OF THIS PAGE *(When Data Entered)*

Constant temperature molecular dynamics calculations of a simple model of a charged metal electrode immersed in electrolyte show the following features known to exist experimentally : incipience of a compact layer, formation of a diffuse layer, presence of highly oriented water layer next to the metal, penetration of nominally diffuse layer species into inner Helmholtz region, ion pair formation between contact adsorbed ion and diffuse layer ion. All these effects emerge from calculations with the same basic model when either the electrolyte composition or the electrode charge are changed. The systems studied had the general composition nI^-+mLi^++(158 - n - m)H_2O where (n,m) = (0,0), (1, 0), (0, 1), (1, 1), and (2, 1). The simulation cell had one metal electrode and one constraining dielectric surface. The surface charge on the metal was q_M=0,±e the latter corresponding to electric fields of about ±5×10^7 V/cm. Net charge in aqueous phase fixed at q_{Aq}=-q_M The st2 water model and parameters for lithium iodide were used in the calculations. The temperature was 290K. The fast multipole method for long range coulomb interactions was used to calculate all electrical forces. This is the first application of molecular dynamics combined with the fast multipole method to study properties of electric double layers at a metal surface.

MOLECULAR DYNAMICS MODELING OF ELECTRIC DOUBLE LAYERS

James N. Glosli and Michael R. Philpott
IBM Research Division, Almaden Research Center
650 Harry Road, San Jose, CA 95120-6099

Constant temperature molecular dynamics calculations of a simple model of a charged metal electrode immersed in electrolyte show the following features known to exist experimentally : incipience of a compact layer, formation of a diffuse layer, presence of highly oriented water layer next to the metal, penetration of nominally diffuse layer species into inner Helmholtz region, ion pair formation between contact adsorbed ion and diffuse layer ion. All these effects emerge from calculations with the same basic model when either the electrolyte composition or the electrode charge are changed. The systems studied had the general composition nI^-+mLi^++(158 - n - m)H_2O where (n,m) = (0,0), (1, 0), (0, 1), (1, 1), and (2, 1). The simulation cell had one metal electrode and one constraining dielectric surface. The surface charge on the metal was q_M=0,±e the latter corresponding to electric fields of about $\pm 5\times10^7$ V/cm. Net charge in aqueous phase fixed at $q_{Aq}=-q_M$ The st2 water model and parameters for lithium iodide were used in the calculations. The temperature was 290K. The fast multipole method for long range coulomb interactions was used to calculate all electrical forces. This is the first application of molecular dynamics combined with the fast multipole method to study properties of electric double layers at a metal surface.

INTRODUCTION

This paper describes exploratory molecular dynamics simulations of electric double layers composed of water and monovalent ions adjacent to a metal surface modeled by a Lennard-Jones 9-3 potential and an image potential. The goal of this work was not to describe a particular electrochemical system in great detail, rather it was to determine whether a broad range of double layer phenomena (1, 2) were accessible to simulation using simple models based on the parameters that described bulk properties. For this reason we did not seek to model any particular metal surface, but rather chose only to imbue our model with minimum characteristics of a metal. In choosing ions we selected for known extremes of behaviour. Lithium ion was chosen because it is strongly hydrated and does not normally contact adsorb (same as physisorb) on noble metal electrodes (1). Consequently lithium ion is expected to be confined to the diffuse part of any electric double layer that forms. Iodide was chosen because it does contact adsorb and could participate in any compact layer that formed next to the electrode. These attributes of the st2 model Li and I ions were demonstrated by Glosli and Philpott (3, 4) for charged dielectric electrodes. In calculations with ions adjacent to metals electrostatic interactions can

be large and long ranged due to the large dipole constituted by the ion and its image. Consequently when large scale interfacial structures organize in ionic systems it is imperative that the 'electrostatics' be calculated efficiently and with sufficient accuracy. For this reason we use the fast multipole method (fmm) of Greengard and Rokhlin (5), described briefly in a companion paper (6), to calculate the electrostatic interactions thereby avoiding the use of cut-offs, reaction fields and the like.

What is remarkable about the results of the calculations reported here is that systems with a few independent ions display the richness of features found experimentally. Beyond the scope of this present report is an in depth study of concentration effects. We describe only some preliminary work on effects accompanying an increase in electrolyte concentration. This section is concluded with a brief summary of previous studies in this area. There have been simulations of films of pure water between uncharged dielectric walls (3, 7-9), and charged dielectric walls (3, 4, 10, 11). Some of this work is noteworthy because of a predicted phase transition (10, 11). There have been numerous reports for uncharged metal walls (12-16), (17-20), including one for jellium (18) and several for corrugated platinum surfaces (15-17, 19, 20) predicting water at on top sites oxygen down on Pt(111) and Pt(100). There have also been some for electrolyte solutions between uncharged and charged dielectric walls (3, 4, 21, 22) emphasizing spatial distributions and hydration shell structure. There have been studies for electrolytes between uncharged metal walls (15, 23, 24). The work of Rose and Benjamin (24) is particularly interesting because umbrella sampling was used to calculate the free energy of adsorption. Finally we mention the studies of water between charged metal walls (25), and electrolytes between charged metal walls (25). In a lot but not all of this work the long range coulomb interactions were treated in an approximate way. The exceptions relied on the Ewald method or some modification. However the question of full image inclusion and the shape of the containing boundary has to be resolved even in some of these studies. Spherical boundaries are not appropriate for systems with a slab geometry. For the slab one has to perform the conditionally convergent Coulomb sums in a manifestly plane wise fashion (26). This is a old problem that has occurred in other areas of physics in connection with long range electromagnetic fields inside samples of arbitrary shape. It will not be discussed further here.

THE MODEL

The immersed electrode was modelled as follows. Integral charge in the aqueous phase $q_{Aq'}$ was exactly balanced by charge on the metal q_M. This is an essential constraint of our immersed electrode model. The advantage of the model is we have less than half the number of water molecules needed to simulate a system with two metal electrodes. The metal was represented by two linearly superimposed potentials. Pauli repulsion and dispersive attractive interactions were represented by a 9-3 potential, and the interaction with the conduction electrons by an image potential. In the calculations described here the image plane and origin plane of the 9-3 potential were coincident. This was tantamount to choosing the image plane and the nuclear plane of the metal surface to be coincident. This was acceptable in our scheme because the Lennard-Jones core parameters σ are all large and the 'thickness' of the repulsive wall is also large (ca. 0.247 nm). On the other side of the simulation cell the electrolyte solution was constrained by the 9-3 potential of the second bounding surface (1.862 nm from the image plane of the metal). We refer to the second surface as a dielectric surface, it's main role was to limit the extent of the fluid phase and thereby make the calculations tractable. The simulation cell

was a cube with edge 1.862nm. It was periodically replicated in the xy directions parallel to the electrode surface plane. In summary of what's right with the model can be listed briefly. Long range coulomb interactions were included in essentially an exact way since all images generated by the metal surface were counted. The average 'mean field' molecular polarizabilities that get bulk properties right were included in the parameters defining the water model. Important effects omitted in this treatment: metal surface topology especially different sites, molecular polarizabilities, and molecular distortions.

In all the calculations reported here we use the parameters of the Stillinger (27, 28) st2 water model and the interaction parameters with Li and I ions developed by Heinzinger and coworkers (29). The st2 water molecule model consists of a central oxygen atom (O_st2 or O for short) surrounded by two hydrogen atoms (H_st2 or H for short) and two massless point charges (PC_st2 or PC for short) in a rigid tetrahedral arrangement (bond angle = $\cos^{-1}(1/\sqrt{3})$). The O-H and O-PC bond lengths were 0.10 nm and 0.08 nm respectively. The only Lennard-Jones 'atom' in st2 model is the oxygen atom. The hydrogen H_st2 and point charges PC_st2 interact with their surroundings (i.e. other atoms and surfaces) only via Coulomb interactions. Their charges are q_H=0.23570|e| and q_{PC}=-q_H. The O atom has zero charge. The Li and and I ions were treated as non-polarizable Lennard-Jones atoms with point mass and charge. The atom-atom interaction parameters are taken from Heinzinger's review (29). The (ε,σ) pairs are (0.3164, 0.3100), (0.1490, 0.2370) and (0.4080, 0.5400) for O_st2, Li ion and I ion respectively. The units are ε in kJ/mole and σ in nm . The usual combining rules were enforced for unlike species, namely: $\varepsilon_{AB} = (\varepsilon_{AA}\varepsilon_{BB})^{1/2}$ and $\sigma_{AB} = \frac{1}{2}(\sigma_{AA} + \sigma_{BB})$. The switching function interval ends R_L^{IJ} and R_U^{IJ} all vanish except for st2/st2 pairs, where $R_L^{ST2,ST2}$=0.20160 nm and $R_U^{ST2,ST2}$=0.31287 nm.

The atom-surface interaction parameters were those used by Lee at al (7), A=17.447x10^{-6} kJ(nm)^6/mole and B=76.144x10^{-3} kJ(nm)^3/mole for O, I ion and Li ion. The A and B parameters for H_st2 and PC_st2 were set to zero. The potential corresponding to these parameters describe a graphite-like surface. The Coulomb interaction between molecules was represented as sum of $1/r$ interactions between atomic point charges. These interactions were softened for small molecular separation in the established manner (7) by a switching function S . As already mentioned the short range part of the intermolecular interaction was modeled by Lennard-Jones potential between the atoms of each molecule. All molecule-molecule Lennard-Jones type interactions were cut-off in a smooth fashion at a molecular separation $R = 0.68$ nm by a truncation function T . The atoms of each molecule also interacted with the surfaces at $z = \pm z_o$ where z_o = 0.931 nm. Both surfaces were treated as flat featureless plates with a uniform electric charge density of σ on the metal plate at $+z_o$. This gave rise to a uniform electric field, $E = 4\pi K\sigma$, in the z-direction where

K the electrostatic coupling constant had the value 138.936 kJ.nm/(mole.e^2) in the units used in this calculation. Recall total charge on the electrode was $q_M/e = 0, \pm 1$. The complete interaction energy U is,

$$U = \sum_{\substack{\beta \in A_j \\ i<j}} \left(\left\{ \frac{K q_\alpha q_\beta}{r_{\alpha\beta}} \left[S(R_{ij}, R_L^{ij}, R_U^{ij}) - 1 \right] + 4\varepsilon_{\alpha\beta} \left[\left(\frac{\sigma_{\alpha\beta}}{r_{\alpha\beta}} \right)^{12} - \left(\frac{\sigma_{\alpha\beta}}{r_{\alpha\beta}} \right)^{6} \right] \right\} T(R_{ij}) + \frac{K q_\alpha q_\beta}{r_{\alpha\beta}} \right) \qquad [1]$$

$$+ \sum_\alpha \left\{ - q_\alpha E z_\alpha + \left(\frac{A_\alpha}{(z_\alpha + z_o)^9} - \frac{B_\alpha}{(z_\alpha + z_o)^3} \right) + \left(\frac{A_\alpha}{(z_\alpha - z_o)^9} - \frac{B_\alpha}{(z_\alpha - z_o)^3} \right) \right\}$$

where i and j were molecular indices, and, α and β were atomic indices. The symbol A_i represented the set of all atoms of molecular i . The symbol R_{ij} was the distance between the center of mass of molecules i and j. The symbol $r_{\alpha\beta}$ was the distance between atoms α and β. For small R we followed the practice of modifying the the coulomb energy between st2 molecules and ions by the switching function $S(R, R_L, R_U)$ given by,

$$S(R, R_L, R_U) = \begin{cases} 0 & R < R_L \\ \dfrac{(R - R_L)^2 (3R_U - 2R - R_L)}{(R_U - R_L)^3} & R_L < R < R_U \\ 1 & R_U < R \end{cases} \qquad [2]$$

The values of R_L and R_U were dependent on the types of the molecular species that were interacting.

As mentioned above the tails of the Lennard-Jones pair interactions were cut off by the truncation function T. The form of T was given by,

$$T(R) = \begin{cases} 1 & R < R_L^T \\ \left(1 - \left(\dfrac{R - R_L^T}{R_U^T - R_L^T} \right)^m \right)^n & R_L^T < R < R_U^T \\ 0 & R_U^T < R \end{cases} \qquad [3]$$

The same truncation function has been applied to all non Coulombic molecular interactions, with R_L^T=0.63 nm and R_U^T=0.68 nm. The integers m and n controlled the smoothness of the truncation function at R_L^T and R_U^T respectively. In this calculation $n = m = 2$ which insured that energy was smooth up to first spatial derivatives.

Bond lengths and angles were explicitly constrained by a quaternion formulation of the rigid body equations of motion (30). The equations of motion were expressed as a set of first order differential equations and a fourth order multi-step numerical scheme with a 2 fs time step was used in the integration. At each time step a small scaling correction was made to the quaternions and velocities to correct for global drift. Also the global center of mass velocities in the x and y directions was set to zero at each time step by shifting the molecular translational velocities.

ELECTRODES IMMERSED IN ELECTROLYTE

This section describes briefly our studies of the immersed electrode using the model described in the last section. In the absence of ions 158 water molecules corresponded to about 4.5 layers of water. The layer was not complete in the sense that in the Lee model (7) the 216 water molecules organized roughly into six layers. Most of the simulations were run for 100 ps to anneal the film and then for a further 900 ps to gather configurations used in the construction of the density profiles shown in the figures. The density plots in Figures 1 and 2 used configurations stored every 1.0 ps. The density plots in Figures 3 to 6 used configurations stored every 0.5 ps.

158 st2 Waters. Immersed Metal Electrode

Uncharged Electrode. Figure 1 displays water component (molecule center of mass H_2O, proton H_st2, and point charge PC_st2) density profiles $\rho(z)$ for 158 st2 water molecules averaged in the xy plane with a bin size of 0.005 nm. The simulation time was 0.9 ns with configurations stored every 1 ps. There are four clearly visible peaks in H_st2, PC_st2 and H_2O, with some 'pile up' at the walls. Compared to the previous calculations of Glosli and Philpott (3, 4) the presence of the metal's image plane has almost no effect on the densities. The charge density shows weak positive deviations from zero at the boundaries due to the longer length of the O-H bond (0.1 nm) compared to the O-PC bond (0.08 nm). Qualitatively this appears little different from the two dielectric surface (3) result.

Anodically Charged Electrode. The results for field on resemble those published earlier for 216 st2 water molecules (3) in a weaker field of $2x10^7$ V/cm (equivalent to 0.11 e/(nm)^2). In the current simulation the field is about three times stronger and the film effectively 0.3 nm thinner. Figure 2 shows the density profiles for a field that repelled protons away from the metal. Notice that there is an overall loss in structure in the water density, which appeared distinctly flatter than the corresponding profile in zero field (compare Figure 1). There was a distinct peak at the dielectric surface for H_st2 atoms that caused the left hand peak in the charge density. There was about 1.7e of charge in this peak and about -0.5e units in the adjacent negative going peak due to PC_atoms in the the first layer of water at the dielectric electrode. This negative charge comes from the main peak in the PC_density profile at -0.65 nm. At the metal electrode the oscillation in the charge density was less pronounced but qualitatively the same. The minimum at 0.75 nm was due to the distinct shoulder in the PC atom density and the peak at 0.6 nm was due to main peak in the H atom density at about 0.6 nm (see Figure 2).

In agreement with the earlier study, we see in the charge density a region that over compensated the charge next to the surface followed immediately by a layer of charge of opposite sign that in turn partially compensated the first. These layers were closer together than the diameter of a water molecule and were due to closer packing of water molecules at the surface. This packing was the result of partial breaking of H-bonds by the applied electric field and 9-3 surface field.

I^- and 157 Waters. Compact Layer on an Anodically Charged Metal

Iodide represents one extreme case of adsorption. Experimentally iodide is known to contact adsorb, in contrast to hydrated lithium ion which does not. The simulation cell contained one iodide ion and 157 st2 water molecules. In this simulation the field across the system was an attractive field for anions equivalent to that generated by -1 unit of electronic charge smeared uniformly over the z=+0.931 nm plane. Figure 3 shows density profiles for all the components of the system as a function of distance across the gap. The bin size used in accumulating the densities was approximately 0.005 nm.

The high field behaviour of one iodide ion in 157 waters was found to be similar to that found previously for iodide in LiI and 214 waters between charged dielectric electrodes (3, 4). Basically the iodide distribution here consisted of one sharp peak indicating that the ion spends almost all its time at the repulsive wall boundary of the metal, and this high field behaved like a strong contact adsorber. The narrowness of the distribution indicated that only short time excursions were made away from the surface. Figure 3 shows it to be rarely removed more than 0.1 nm from contact. The anion density profile was sharply peaked at z = 0.700 nm very close to the beginning of the repulsive wall at 0.684 nm. The point of closest approach was about 0.74 nm, and that farthest retreat was about 0.65 nm. In the charge density profile the iodide contributed a sharp negative peak on top of a rather broad negative density region centered around 0.72 nm due to the PC atoms of the first layer of water. We discuss this water layer next.

There was significant structure in water, H and PC densities near the metal boundary. The water density displayed four pronounced maxima and one minimum (see Figure 3): narrow peak at -0.67 nm due to water pile up at the dielectric boundary, a broad peak at 0.28 nm followed by an equally broad minimum at 0.43 nm likely due to water exclusion from the vicinity of iodide due to it's size, a peak at 0.56 nm due to 'non oriented surface water' and a sharp peak at 0.66 nm due to highly oriented surface water with one PC atom pointed directly at the metal.

This last feature must along with the sharp iodide peak be considered a key feature of the inner region of the double layer. The strongly oriented layer of surface water one molecule thick occurred when the applied field and anion and image field reinforced. The two peaks at z = 0.74 and 0.63 nm (δz = 0.11 nm) in the PC density arose from the negative charge on the same molecule, one pointing directly at the metal and the other away at the tetrahedral angle. The surface peak in the H density at 0.62 nm was approximately twice the area (over background) but at same position, clearly indicating that it belonged to the same highly oriented surface layer.

The PC density as mentioned already had two components near the surface. The peak at 0.74 nm contributed approximately -1.5|e| to the total negative charge (about -2.5|e|) in the large negative peak in the total charge density at 0.70 nm. Between -0.6 nm and 0.4 nm the H and PC densities are computed to be almost identical, so that this region was always neutral. Comparing the charge densities of pure water and this system we see that the presence of the ion and it's image created extensive polarization of the water. The metal boundary showed strong polar regions with alternating sign extending to out z = 0.2 nm as a result of water structure resulting from shielding of the fields of the charged electrode, adsorbed iodide ion, and the first layer of oriented water.

Li^+ and 157 waters. Diffuse Layer on a Cathodically Charged Metal

Figure 4 shows density profiles of the single lithium ion (normalized to unity), 157 waters, H and PC components, and the charge density across the system with a bin size of 0.005 nm. The density plots in this Figure used configurations from 100 ps to 1000 ps, stored every 0.5 ps.

In this simulation the field was reversed, the charge on the metal being -1.0el, so that the positive ion was attracted to the metal on the right side of the figure. First thing to notice is the over all similarity to Figure 3 in the water, H and PC profiles except that the profiles for H and PC are reversed in the case of Li compared to I due to change in field direction. This means that there was a highly oriented layer of surface water with protons H pointing directly at the metal. This reversal was of course quite consistent given the reversal in the field and the fact that the direction of ion field and that of it's image were also reversed. The peak heights were larger in the present case for three reasons. First the protons H_st2 could get closer to the image plane than in the case of PC_st2 because O_H bond was longer. Second the field of the Li ion and its image was spread over a larger area of the electrode because it is located further from the electrode. Third the Li ions primary hydration shell penetrates to the wall and contributes localized water to the distributions.

The density profile for Li defines a bimodal diffuse region between -5.5 and 5.5 nm with a minimum at 0.15 nm. Throughout this region the total charge was mostly zero. The distance of closest approach to the hard wall of the metal was approximately 0.13 nm or the radius of a water molecule. At this extremum the primary hydration shell of the lithium ion has to be mixed in with the highly oriented layer of water at the surface. The positive ion felt the influence of its image and was 'splayed' against the hard wall thereby affording a further reduction in the distance of approach to less than $0.5(\sigma_{Li}+\sigma_O)$. Glosli and Philpott (3, 4) have discussed the adsorption of hydrated ions and their possible distances of approach. At the minimum of the bimodal Li ion distribution the distance from the hard wall was approximately 0.54 nm, which should be compared with 0.60 nm the distance corresponding to separation from the wall by two water molecules. The interpretation of the Li distribution now seems clear. The peak between -0.55 and 0.15 nm is most likely a diffuse layer component with distance of closest approach being the outer Helmholtz plane, whilst the somewhat weaker diffuse-like component closer to the metal represents the smaller statistical probability of penetrating past the outer plane into the inner layer. This latter process depends strongly on the exact nature of the forces acting at the surface (crystal plane sites, size of the ion, etc.) and in some experimental systems and might well be absent altogether. What is important here is the idea that nominally diffuse layer ions can penetrate the outer plane and comingle with inner layer species. As mentioned already the ability of an ion to do this will depend critically on double layer structure and topography of the electrode surface.

Li^+, I^- and 156 Waters. Weakly Oriented Water at the PZC

In this simulation the applied field was zero so there was no charge on the metal electrode. In some ways this case mimics the potential of zero charge (pzc). The main electrostatic fields are now amongst the charges making up the ions and water and their images in the metal surface at z = 0.931 nm. Figure 5 displays the density profiles for water, protons H_st2, point charges PC_st2, each ions and the total charge density as a function of position across the film.

Some of the features were similar to those discussed already. Emphasize here is on major points of difference. The surface electric fields due to ions and their images were weaker since there was no net applied field and the image fields of the ions tend to cancel on the average. We note first of all that all the water related densities were flatter across the whole film, the H and PC surface peaks appear only as shoulders, just as in the case already examined of water in zero field. This means that first layer of water was not well oriented as in the previous two examples. This is of course consistent with the experimental finding that at the pzc water is less well bound. Consistent with this conclusion was the observation that the charge density was positive at the extreme edge of the film. This is consistent with the known result for water without ions (3) and the charge profile displayed in Figure 1.

Note that the iodide density has a tail not present in any of the simulations with non-zero fields, that overlaps the tail of the Li ion distribution. This was a new feature that signals the possible formation of temporary ion pairs in the double layer. In this case the contact adsorbed ion attracted compensating ion of opposite sign from out of the diffuse layer. In the present case the separation between iodide peak and nearest Li peak was approximately 0.55 nm. This would seem to rule out an ion pair configured with nuclei along the surface normal with interposed water molecule from the primary solvation shell of the cation. This configuration would require a separation of 0.7 nm for all centers to be colinear.

That this interaction could locally alter the diffuse layer can be seen by comparing the diffuse regions of Li ion in Figure 4 with that shown in Figure 5. The idea of altering the position of the outer plane to change the field across the inner layer has been proposed many times. We cite only one example from our own experimental work (31). References to the work of Bewick can be found there. Clearly this phenomenon could be studied further even with the primitive model used here.

The minimum in the bimodal Li ion distribution was at approximately -0.1 nm. At this position the Li ion was separated from the hard wall by 0.784 nm, much more than two water molecules. At the pzc the Li ion was not bound by a charge originating on the metal. It was bound by the field of the contact adsorbed species and its image. Since this was a dipole field the attraction between the iodide and lithium ions was weak. The Li ion in the density between -0.55 and -0.10 nm may be metastable and may well displace to larger separations if the water film were thicker.

Li^+, two I^- and 155 waters. Diffuse and Compact Layers

In this simulation there was a field of approximately $5x10^7$ V/cm attracting negative ions to the metal. Figure 6 displays the density profiles for all components of the system and the charge density. The simulation time was 1000 ps with the first 100 ps discarded for equilibration, configurations were stored every 0.5 ps.

Note that both iodide ions were adsorbed in a sharply peaked distribution that resembled the single adsorbed iodide distribution in Figure 3 than the iodide distribution with the tail seen in Figure 5 of the last section. The single Li ion occupies a (possibly weakly bimodal) diffuse-like distribution between -0.6 nm and 0.3 nm. At large negative z this distribution has a gradually fall off that would be expected for an electrostatically bound species. In contrast the tail of Li ion in Figure 4 drops quickly suggesting it was modified by the presence of the confining dielectric wall. On the positive side the main component of the distribution ends at 0.05 nm. This latter position was 0.63 nm from the hard wall, and was roughly at the same place for the outer plane of Figure 4. The region between 0.05 and 0.3 nm defines, as in Figure 4, the region of greatly reduced probability of penetrating into inner layer and contacting the adsorbed iodide ions.

It was noticeable that the water structure near the metal surface was less well defined than for either a single iodide or a single lithium ion. The reason for this was another new effect, water displacement from the interface as large ions contact adsorb. There was less water to orient next to the metal, and the density profiles mirror this fact.

CONCLUSIONS

In the introduction the question was could the behaviour of molecules and ions near a metal surface be qualitatively modeled with bulk parameters. Broadly speaking the answer appears to be yes. This means that the range of phenomena predicted is consistent with experimental observation. It does not mean that in any specific case we can model detailed behaviour. We have shown how a simple model suffices to reproduce many phenomena familiar from experiments on electric double layers at the electrolyte-metal interface. A key tool was the use of the fast multipole method to accurately and efficiently calculate coulomb interactions so that long range electric fields were computed correctly. This is very important for polar systems. The phenomena described included: contact adsorption of large ions on metals driven by image interactions, diffuse layers of strongly hydrated species, an oriented boundary layer of water next to the electrode when it is charged, relatively poorly oriented water next to uncharged electrode, and a zone of overlap between ions of opposite sign again when the electrode is not charged.

Finally we point out that these calculations suggest that modelling the electrochemical interface can be readily extended to such diverse systems as: nanosized structures, microelectrodes, and polymer coated electrodes. A more detailed analysis of phenomena such as these will be presented elsewhere.

ACKNOWLEDGEMENTS

This research was supported in part by the Office of Naval Research.

REFERENCES

(1) J. O. Bockris and A. K. Reddy, *Modern Electrochemistry, Vol 2* (Plenum Press, New York, 1973).

(2) J. O. Bockris and A. Gonzalez-Martin, *Spectroscopic and Diffraction Techniques in Interfacial Electrochemistry, NATO ASI Series C* (Kluwer,Dordrecht,Holland, 1990), pp 1-54.

(3) J. N. Glosli and M. R. Philpott, J. Chem. Phys. **96**, 6962-6969 (1992).

(4) J. N. Glosli and M. R. Philpott, J. Chem. Phys. **in press**, (1993).

(5) L. Greengard and V. Rokhlin, J. Comp. Phys. **73**, 325-348 (1987).

(6) J. N. Glosli and M. R. Philpott, ECS Symposium Fall 1992 Proceedings, **Toronto**, (1993).

(7) C. Y. Lee, J. A. McCammon, and P. J. Rossky, J. Chem. Phys. **80**, 4448-4455 (1984).

(8) J. P. Valleau and A. A. Gardner, J. Chem. Phys. **86**, 4162-4170 (1987).

(9) Y. J. Rhee, J. W. Halley, J. Hautman, and A. Rahman, Phys. Rev. B **40**, 36-42 (1989).

(10) A. M. Brodsky, M. Watanabe, and W. P. Reinhardt, Electrochimica Acta **36**, 1695-1697 (1991).

(11) M. Watanabe, A. M. Brodsky, and W. P. Reinhardt, J. Phys. Chem. **95**, 4593 (1991).

(12) N. Parsonage and D. Nicholson, J. Chem. Soc. Faraday Trans. 2, **82**, 1521 (1986). pages 1521-1535

(13) N. Parsonage and D. Nicholson, J. Chem. Soc. Faraday Trans. 2, **83**, 663 - 673 (1987). pages 663 - 673

(14) A. A. Gardner and J. P. Valleau, J. Chem. Phys. **86**, 4171-4176 (1987).

(15) E. Spohr and K. Heinzinger, Electrochimica Acta **33**, 1211-1222 (1988).

(16) E. Spohr and K. Heinzinger, Ber. Bunsenges. Phys. Chem. **92**, 1358-1363 (1988).

(17) K. Heinzinger and E. Spohr, Electrochimica Acta **34**, 1849-1856 (1989).

(18) J. Hautman, J. W. Halley, and Y. Rhee, J. Chem. Phys. **91**, 467-472 (1989).

(19) K. Foster, K. Raghavan, and M. Berkowitz, Chem. Phys. Lett. **162**, 32-388 (1989).

(20) K. Raghavan, K. Foster, K. Motakabbir, and M. Berkowitz, J. Chem. Phys. **94**, 2110-2117 (1991).

(21) R. Kjellander and S. Marcelja, Chemica Scripta **25**, 73-80 (1985).

(22) E. Spohr and K. Heinzinger, J. Chem. Phys. **84**, 2304-2309 (1986).

(23) J. Seitz-Beywl, M. Poxleitner, and K. Heinzinger, Z. Naturforsch. **46A**, 876 (1991).

(24) D. A. Rose and I. Benjamin, J. Chem. Phys. **95**, 6856-6865 (1991).

(25) K. Heinzinger, Pure Appl. Chem. **63**, 1733-1742 (1991).

(26) G. E. Schacher and F. W. de Wette, Phys. Rev. **136A**, 78-91 (1965).

(27) F. H. Stillinger and A. Rahman, J. Chem. Phys. **60**, 1545 (1974).

(28) O. Steinhauser, Mol. Phys. **45**, 335-348 (1982).

(29) K. Heinzinger, *Computer Modelling of Fluids Polymers and Solids*, (Kluwer,Dordrecht, 1990), pp. 357-404.

(30) M. P. Allen and D. J. Tildesley, *Computer Simulation of Liquids* (Oxford University Press, Oxford, 1989), pp. 88-90.

(31) K. Ashley, M. G. Samant, H. Seki, and M. R. Philpott, J. Electroanal. Chem. **270**, 349-364 (1989).

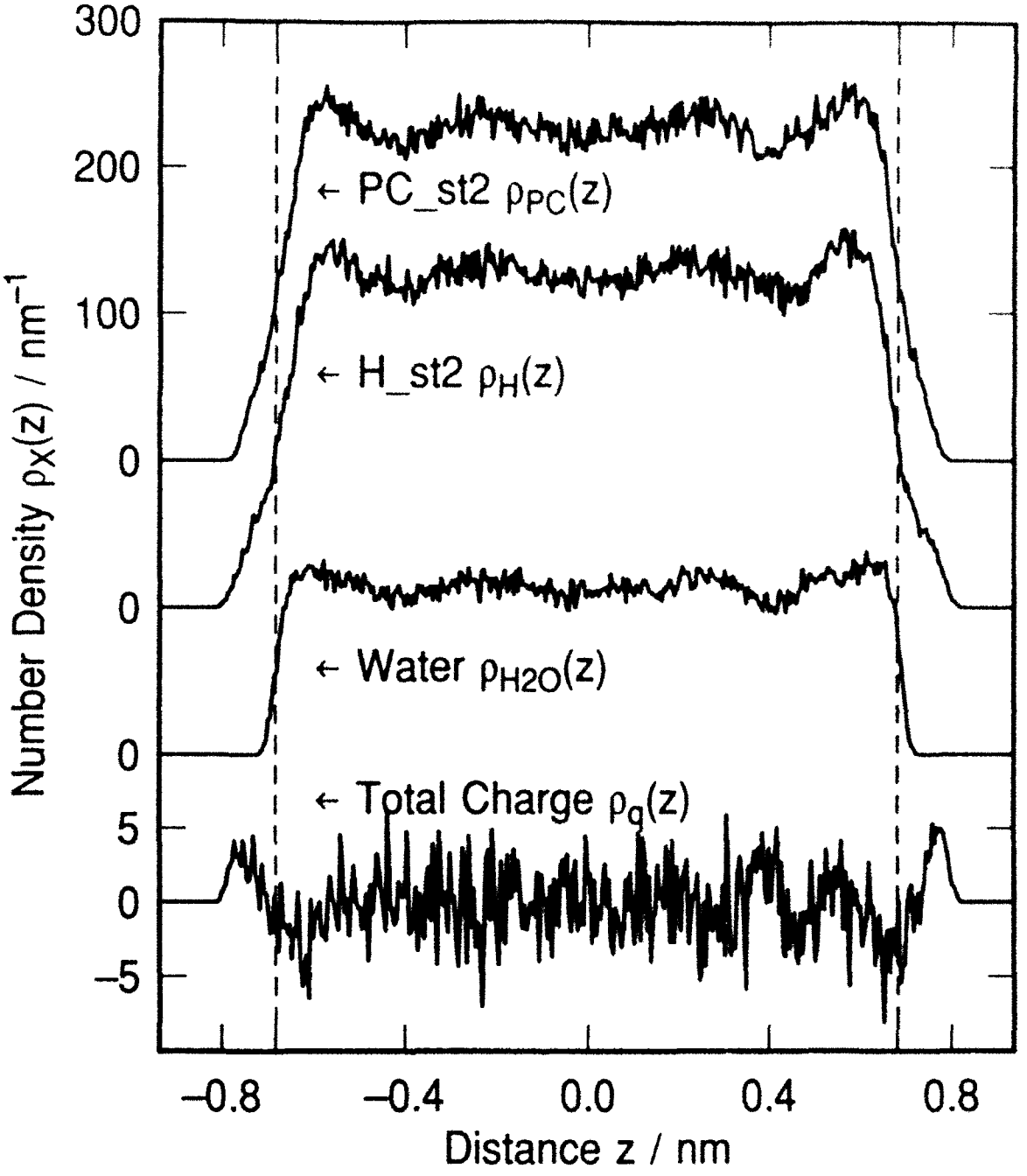

Figure 1. Water in zero field. Density profiles for 158 st2 water molecules adjacent to uncharged metal electrode on right side. Left side confining boundary is a dielectric surface with no image field. Gap between surfaces is Δz = 1.862 nm.

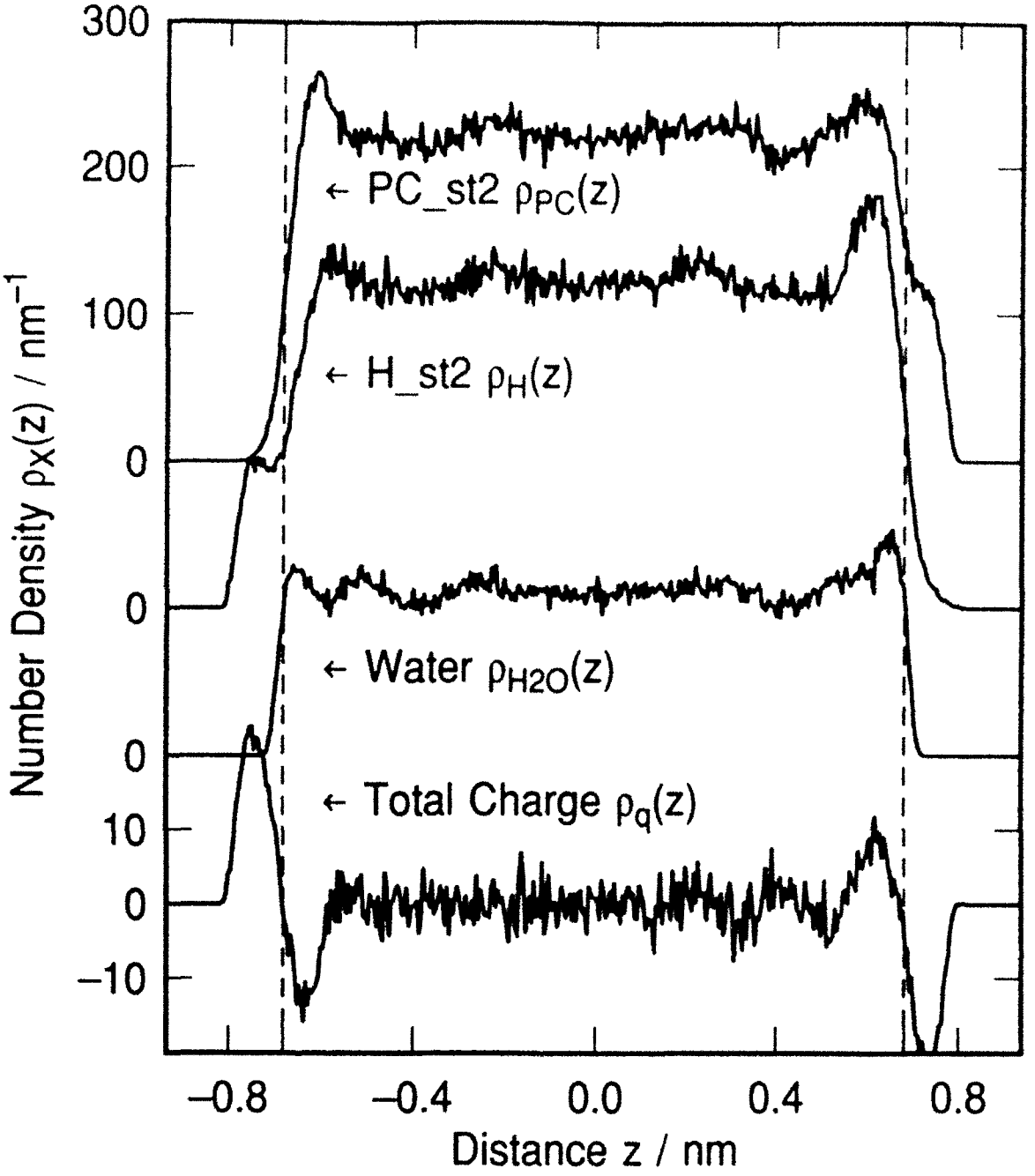

Figure 2. Water in field of 5×10^7 V/cm. Density profiles for 158 st2 water molecules adjacent to charged metal electrode on right side. Right confining boundary is a dielectric surface with no image field. Gap between surfaces is $\Delta z = 1.862$ nm.

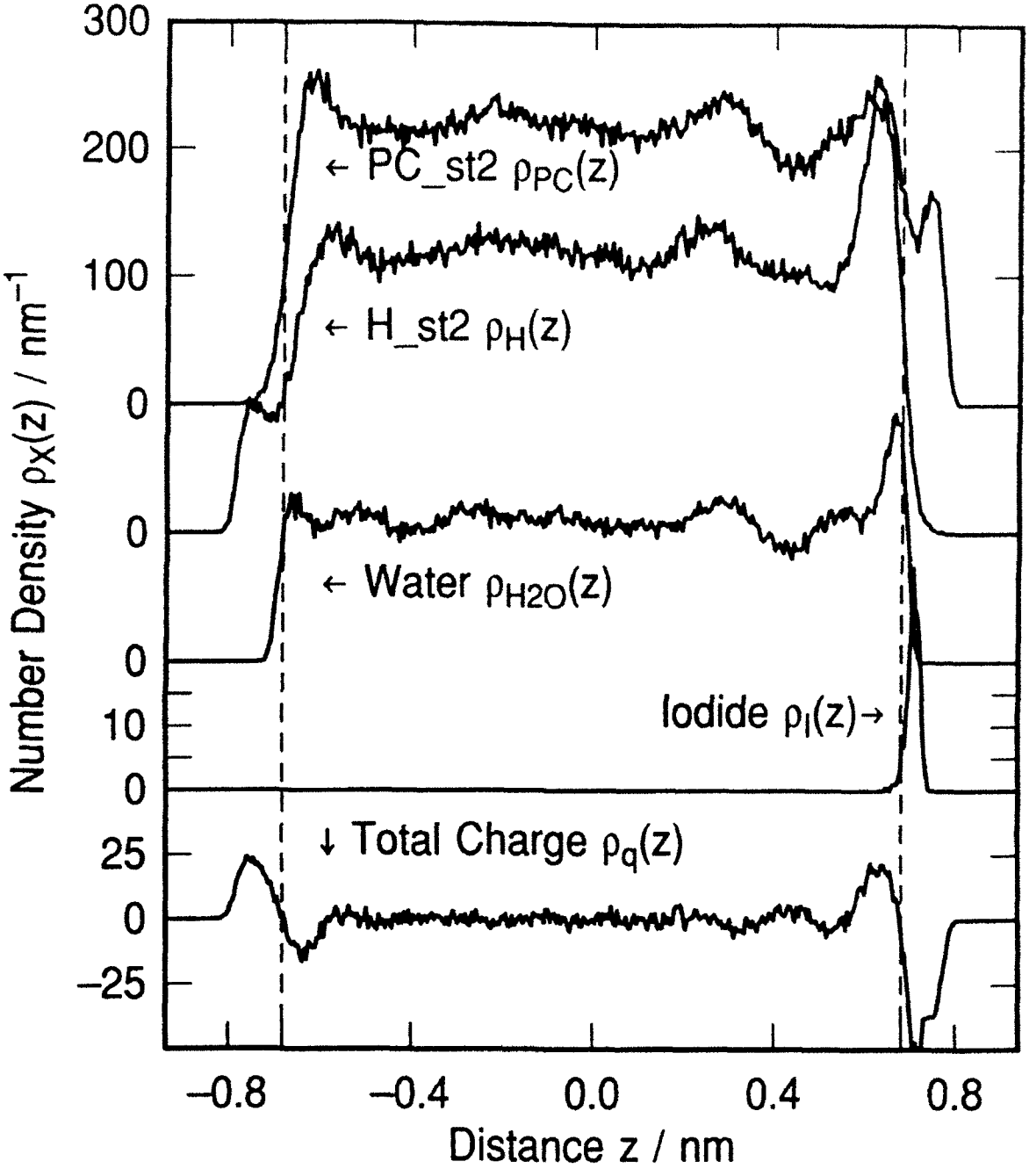

Figure 3. Density profiles for one iodide ion I^- and 157 st2 water molecules between a charged metal electrode and the dielectric boundary. The metal has anodic bias equivalent to a field of 5×10^7V/cm. Image plane at z = 0.931 nm . Repulsive portion of the wall potentials begin at |z| = 0.682 nm.

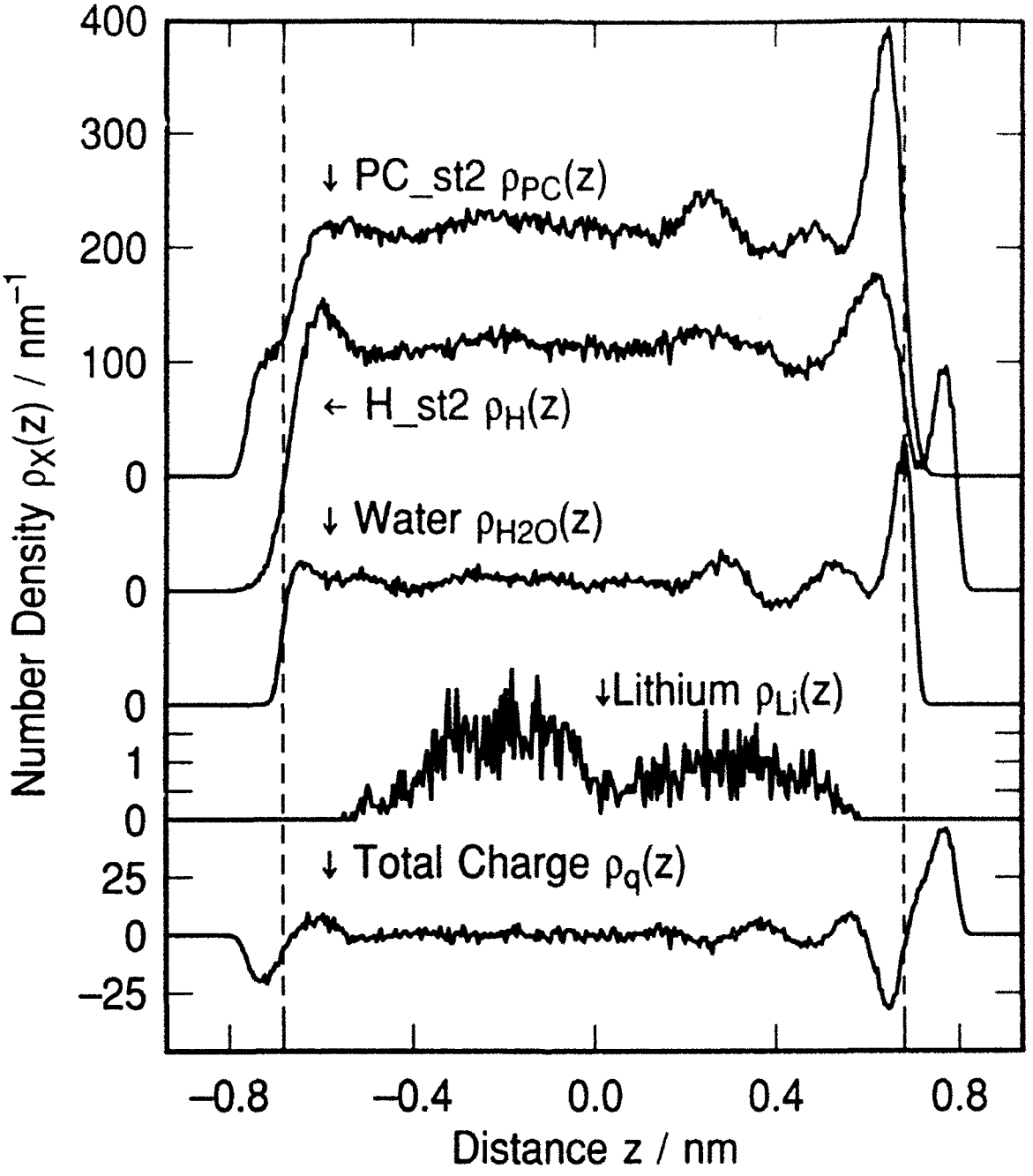

Figure 4. Density profiles for one Li^+ ion and 157 st2 waters near an immersed electrode with cathodic bias. Metal electrode on right hand side, dielectric on the left. Image plane at z = 0.931 nm and repulsive wall at |z|=0.682 nm.

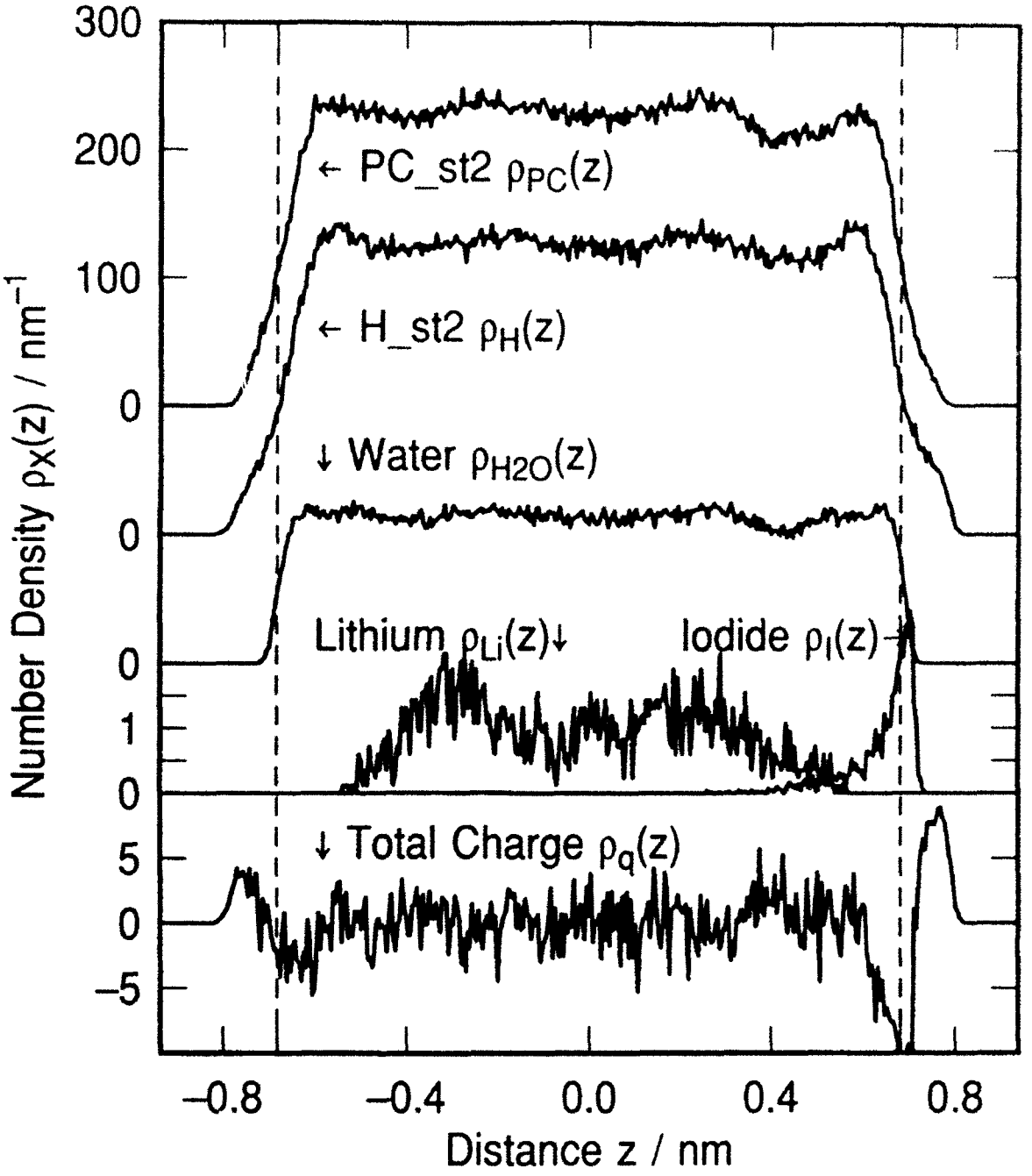

Figure 5. Density profiles for one Li^+ ion, one I^- ion and 156 st2 waters near an uncharged immersed electrode. Metal electrode on right hand side, dielectric on the left. Image plane at z = 0.931 nm and repulsive walls at |z|=0.682 nm.

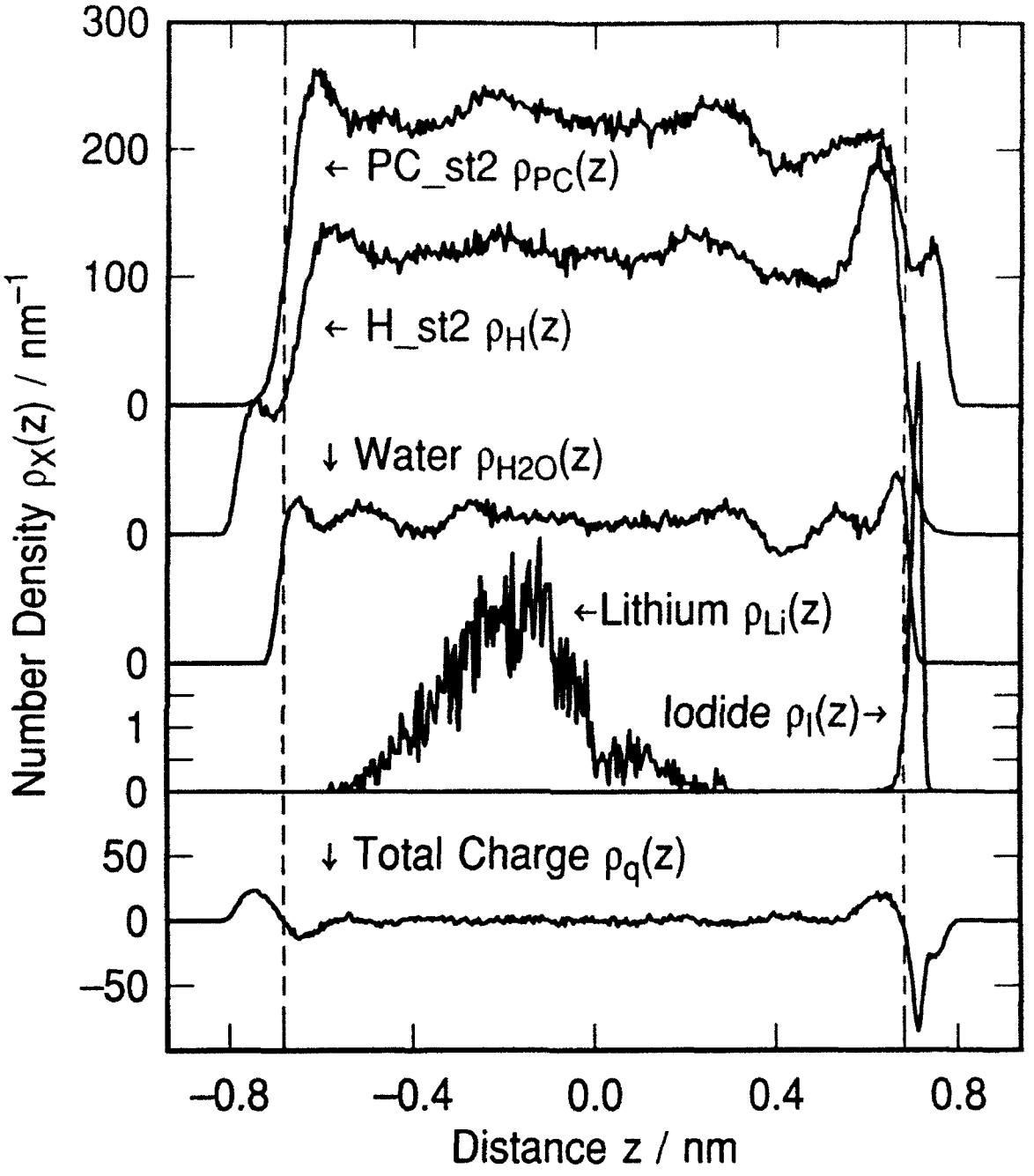

Figure 6. Density profiles for two I^-, one Li^+ and 155 st2 water molecules next to immersed electrode. Anodic bias corresponding to static electric field of 5×10^7 V/cm.